Direct integration of vertical In_2O_3 nanowire arrays, nanosheet chains, and photoinduced reversible switching of wettability

Miao Zhong,[1] Maojun Zheng,[1,a)] Ansheng Zeng,[1] and L. Ma[2]
[1]*Laboratory of Condensed Matter Spectroscopy and Opto-Electronic Physics, Department of Physics, Shanghai Jiao Tong University, Shanghai 200240, People's Republic of China*
[2]*School of Chemistry and Chemical Technology, Shanghai Jiao Tong University, Shanghai 200240, People's Republic of China*

(Received 7 June 2007; accepted 22 January 2008; published online 6 March 2008)

Large-scale In_2O_3 nanowire (NW) arrays and nanosheet chains are directly integrated on InP substrates via a simple chemical vapor deposition process, benefiting from the substrate-induced, self-assembly and self-catalyzed vapor-liquid-solid growth mechanism. Such particular structures could be expected to have potential applications such as gas sensors and field emission devices. Equally important, remarkable photoinduced wettability conversion between superhydrophobicity and high hydrophilicity has been observed on In_2O_3 NW arrays. This reversible behavior is ascribed to the photogenerated surface oxygen vacancies and the special nanostructures. Such reversibly switching surface will widen the applications of In_2O_3 films. © *2008 American Institute of Physics*. [DOI: 10.1063/1.2844855]

It is well known that there is a consistent relationship between specific morphologies of nanostructures and their corresponding unique performance in physics and material science,[1,2] and the latter is the foundation of their future applications. Until now, many methods have been studied for this purpose including high-temperature evaporation,[3] laser ablation,[4] chemical vapor deposition (CVD),[5–7] hydrothermal process,[8,9] and anodic aluminum oxide templating.[10,11] In this letter, a facile and controllable approach is presented for fabrication of large-scale vertical nanowire arrays and nanosheet (NS) chains. Equally important, tunable wettability of vertical In_2O_3 nanowire (NW) arrays has been observed by UV illumination, which is considered as the combined effect of surface photosensitivity and special nanostructures of the films.[12–17] Such special wettability will widen the applications of In_2O_3 films to other important fields such as intelligent microfluidic devices, fundamental biothecnology, self-cleaning surface, etc.[18–20]

The InP nanopore array substrates were fabricated through an anodizing electrochemical method.[21] Figure 1(a) shows the typical scanning electron microscopy (SEM) (Philips XL30FEG) image of InP nanopore arrays. The average inner diameter (diagonal length) of nanopores and the average wall thickness between nanopores were estimated to be 120 and 75 nm, respectively. The subsequent CVD processes are briefly discribed as follows. Different substrates (with indium source) loaded in a ceramic boat were placed into the center of a horizontal quartz tube. First, the tube was evacuated for 10 min by mechanical pump. Then, the temperature of the tube was increased to 450/600 °C in 30 min, maintained at this temperature for a certain time and then naturally cooled down to room temperature. Pure O_2 was kept flowing into the tube during the whole process at a rate of 80 SCCM. (SCCM denotes standard cubic centimeter per minute at STP). Finally, large-scale In_2O_3 nanostructures were obtained. This process has been repeated for several times and good reproducibility is observed.

The growth conditions of vertical In_2O_3 NW arrays are as follows: porous InP substrates and annealing temperature of 450 °C for 2 h. Figure 1(b) demonstrates that vertical In_2O_3 NWs are dispersedly aligned in a high yield, with the diameters around 90–120 nm and the length around 2–5 μm. Figure 1(c) is a high-magnification SEM image of a single NW from which axial screw dislocations could be clearly observed. To further investigate the growth mechanism, we cut off the supply of O_2 at 300 °C during the cooling step while kept the other conditions unchanged. The corresponding SEM image is shown in Fig. 1(d). Obvious dropletlike configuration can be seen on the tip of each NW. Furthermore, transmission electron microscopy (TEM) (JEOL JEM-2100F) and high-resolution TEM (HRTEM) were employed to observe this interesting structure. Figure 1(e) shows a TEM image of a single NW with a similar dropletlike morphology at its tip. The selected area electron diffraction (SAED) pattern of the body area of the NW [lower right image of Fig. 1(e)] indicates that it is single-crystalline In_2O_3 and is grown along the (100) direction. The corresponding HRTEM image [upper right image of Fig. 1(e)] further shows that the lattice fringes are spaced 0.2530 nm (vertical direction) which agrees with the (400) plane of In_2O_3 crystal. Energy dispersive x-ray (EDX) analysis result [Fig. 1(f)] reveals that the atomic ratio of In/O is 60.1:39.8 at the tip area, which implies that excessive indium exists. We suppose that the tip area should be eutectic state of In and In_2O_3 during the growth process.

It is generally accepted that the growth of NWs is usually based upon three models: vapor-liquid-solid (VLS), vapor-solid, or conventional spiral growth mechanism.[22–24] In VLS model,[25,26] an intermediate nanoparticle is always located at one end of the nanowire to serve as catalyst between the vapor feed and the solid growth. Taking into account all the evidences, it is concluded that NWs grow along the axial screw dislocation layer by layer via self-catalyzed VLS mechanism.

The evolution of vertical In_2O_3 NW arrays is complicated. In brief, it involves two fundamental steps: decomposition and nucleation. When the furnace temperature was increased to 450 °C, a great mass of porous InP surface

a)Author to whom correspondence should be addressed. Electronic mail: mjzheng@sjtu.edu.cn

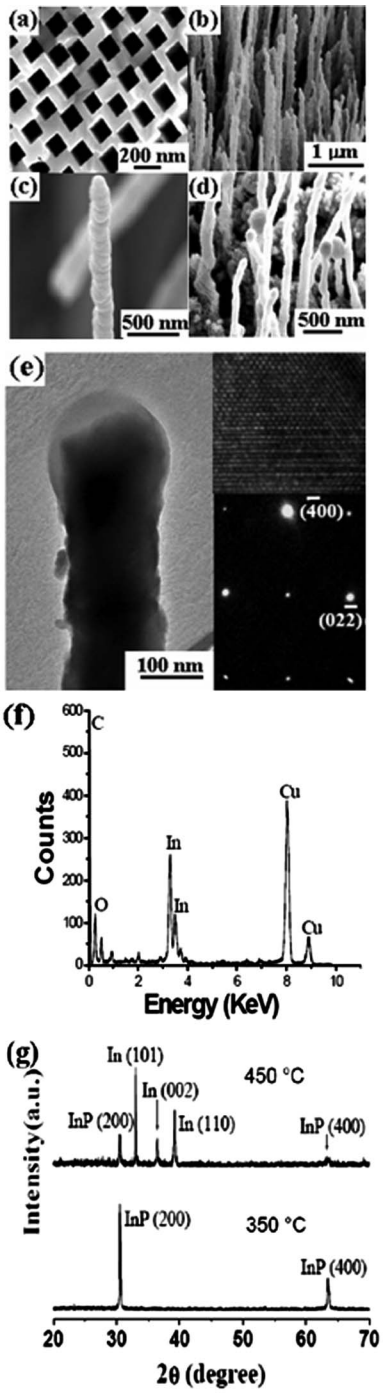

FIG. 1. (a) SEM image of InP nanopore arrays. (b) SEM image of vertical In_2O_3 NW arrays. (c) SEM image of single In_2O_3 NW. (d) SEM image of the In_2O_3 NWs with obvious dropletlike morphology at the tips. (e) TEM image of single In_2O_3 NW, the insets on the right are the corresponding SAED pattern and HRTEM image. (f) EDX pattern of tip area of single NW. (g) The x-ray diffraction (XRD) pattern of porous InP annealed in the vacuum chamber at 350 and 450 °C for 2 h.

decomposed into phosphorus and indium, which was proved by the typical x-ray diffraction (XRD) spectra results (Bruker D8 ADVANCE system) shown in Fig. 1(g). Phosphorus vapor was extracted away by the vacuum pump. Indium (as a reactant) captured O_2 to form In_2O_3 nuclei to assure the growth of NWs. Indium (also as a catalyzer) diffused into In_2O_3 to form the eutectic so as to facilitate the growth of NWs. These basic actions occurred simultaneously and continuously.

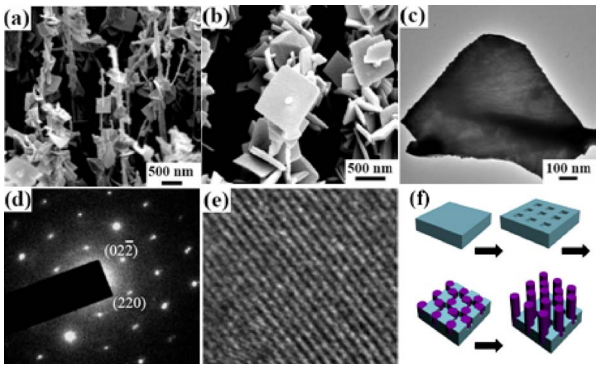

FIG. 2. (Color online) (a) SEM image of dispersive NS chains. (b) SEM image of compacted NS chains. (c) TEM image of single In_2O_3 NS. (d) Corresponding SAED pattern of NS. (e) Corresponding HRTEM of NS. (f) The schematic illustration of growth process of vertical In_2O_3 NW arrays.

A simple model of vertical NW growth is proposed, as shown in Fig. 2(f). We suppose that the decomposition of porous InP substrate began at superficial areas of the nanowall between the pores owing to its higher rate of surface/volume. Then, following the growth mechanism discussed before, vertical NW arrays were obtained. We suggest that the porous structure here plays a crucial role. It could increase the decomposition of InP under lower temperature. Meanwhile, it confines the fluidity of molten indium so that the initial eutectic nuclei form separately on the top of the porous edges, facilitating dispersed In_2O_3 NW growth. In contrast, if we use smooth bulk InP as substrate, the molten indium could mess up together on the surface and the nanostructure can not be obtained. In addition, the porous structure could provide surface stress which could hold the In_2O_3 nuclei erect between the holes and keep the growth direction epitaxial along the porous wall which is perpendicular to the substrate.

Note that many influential factors could determine the results, such as substrate geometry, annealing temperature, time control, use of extra source, etc. NS chains were obtained by altering the conditions purposefully [In_2O_3 NW arrays substrates, extra indium source (0.6 g), annealing temperature of 600 °C for 2 or 4 h]. Figures 2(a) and 2(b) show the SEM images of NS chains. Via 2 h CVD process, NSs started to form and grew on In_2O_3 NWs dispersedly [Fig. 2(a)]. When increasing CVD process to 4 h, NSs accumulated compactly along NWs in large scale like three-dimensional nanonetwork chains [Fig. 2(b)] and the individual NS is mainly thin and a square sheetlike structure. Its side length is approximately between 700 to 800 nm which could be also observed from the TEM image [Fig. 2(c)]. Figures 2(d) and 2(e) show its corresponding SAED and HRTEM patterns which prove In_2O_3 NS is highly single crystalline and grows along the (220) direction.

The growth mechanism of NS chains could be ascribed to combined effect of substrate inducement (dislocation inducement) and self-assembly property. Due to employment of an extra indium source and improvement of growth temperature, indium vapor became supersaturated in the chamber which might greatly enhance the deposition of indium on the spiral dislocations of NWs [Fig. 1(c)] so as to boost nucleation and growth of In_2O_3 along the radial direction.[27,28] Following the self-assembly CVD process, NS chains gradually formed.

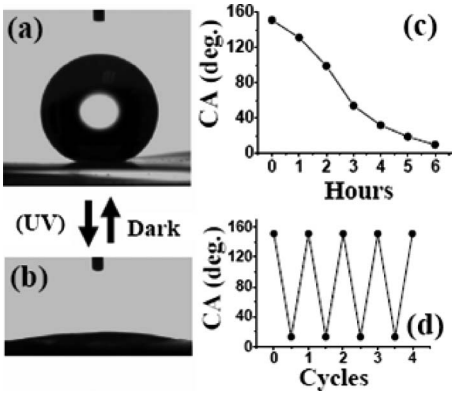

FIG. 3. Photoinduced reversible wettability of In_2O_3 NW arrays [(a) and (b)] Images of water droplet shape before and after UV illumination. (c) Variation of water contact angles with UV illumination time. (d) Reversible wettability conversions via UV illumination and dark storage.

The surface wettability of the In_2O_3 nanowire arrays was investigated by measuring the water contact angle (CA) by an OCA20 contact angle system (Data physics Instrument GmbH, Germany) at ambient pressure and room temperature. Miyauchi *et al.* reported that pure In_2O_3 film with a smooth surface demonstrates a water CA of around 20°.[14] However, the apparent water CA values of the as-prepared In_2O_3 nanowire arrays was 155° shown in Fig. 3(a). It reveals the superhydrophobic behavior. As reported,[12] the nanostructured surface roughness might contain enough room to hold air in the troughs between separately aligned NW arrays on which a water droplet sits. Based on Cassie and Baxter's equation,[29] it is explicit that increasing the proportion of air/water interface will intensify the hydrophobic properties.

UV illumination was carried out using a 150 W Xe lamb with wavelength around 200–400 nm. Figure 3(c) shows that the water CA gradually decreases with the increase of UV illumination time. If UV illumination was longer than 6 h, the water CA deceased to 10°, as shown in Fig. 3(b). After UV illumination, the films were placed in darkness for a certain time (above 12 days), the structure induced superhydrophobicity was obtained again, and the reverse process took place with full reproducibility over several times shown in Fig. 3(d). However, the remarkably photoinduced conversion of wettability does not occur on the smooth surface of In_2O_3 film.[14] According to other reports,[12,15,17] we suggest that the surface roughness in nanoscale could greatly magnify the superficial acreage of In_2O_3 so as to largely increase the chances of generation of electron-hole pairs in the In_2O_3 surface under UV irradiation. Some of the holes could react with lattice oxygen to form surface oxygen vacancies. These defective sites are kinetically more favorable for hydroxyl adsorption, which leads to improved dissociative adsorption of water molecules. Also, due to such special microstructure, water droplet will enter and fill the distant spaces in the films which lead to three-dimensional capillary effect. This effect also enhances the wetting for the hydrophilic surface.[12] Therefore, the wettability conversion under UV illumination could be ascribed to the combined effect of preferential adsorption of water molecules on the photogenerated surface defective sites and three-dimensional capillary of special nanostructure. In addition, this interesting phenomenon does not appear in the as-prepared In_2O_3 nanostructure coated with a thin Au layer on the surface. The Au coated nanostructure demonstrates almost the same water CA of 155° before and after the UV illumination which gives an indirect proof to our supposition.

As reported,[12,17] after storing the sample in dark and air condition for a certain time, defective sites will gradually disappear due to the atmospheric oxygen effect. The surface recovers to the original superhydrophobicity. By the alternation of UV photoinducement and dark storage, the reversible switching of wettability was achieved [Fig. 3(d)].

This work was supported by the Natural Science Foundation of China (Grant No. 50572064) and the National Minister of Education Program for Changjiang Scholars and Innovative Research Team in University (PCSIRT).

[1] J. G. Lu, P. Chang, and Z. Fan, Mater. Sci. Eng., R. **52**, 49 (2006).
[2] P. Nguyen, H. T. Ng, T. Yamada, M. K. Smith, J. Li, J. Han, and M. Meyyappan, Nano Lett. **4**, 651 (2004).
[3] Z. W. Pan, Z. R. Dai, and Z. L. Wang, Science **291**, 1947 (2001).
[4] E. Bakkers and M. A. Verheijen, J. Am. Chem. Soc. **125**, 3440 (2003).
[5] Z. G. Chen, J. Zou, G. Q. Lu, G. Lu, F. Li, and H. M. Cheng, Appl. Phys. Lett. **90**, 103117 (2007).
[6] S. Q. Li, Y. X. Liang, and T. H. Wang, Appl. Phys. Lett. **88**, 053107 (2006).
[7] Y. F. Hao, G. W. Meng, C. H. Ye, and L. D. Zhang, Cryst. Growth Des. **5**, 1617 (2005).
[8] F. Li, Y. Ding, P. X. Gao, X. Q. Xin, and Z. L. Wang, Angew. Chem. **116**, 5350 (2004).
[9] B. Liu and H. C. Zeng, J. Am. Chem. Soc. **125**, 4430 (2003).
[10] M. J. Zheng, L. D. Zhang, G. H. Li, X. Y. Zhang, and X. F. Wang, Appl. Phys. Lett. **79**, 839 (2001).
[11] J. X. Ding, J. A. Zapian, W. W. Chen, Y. Lifshitz, and S. T. Lee, Appl. Phys. Lett. **85**, 2361 (2004).
[12] X. Feng, L. Feng, M. Jin, J. Zhai, L. Jiang, and D. B. Zhu, J. Am. Chem. Soc. **126**, 62 (2004).
[13] R. Wang, K. Hashimoto, A. Fujishima, M. Chikuni, E. Kojima, A. Kitamura, M. Shimohigoshi, and T. Watanabe, Nature (London) **388**, 431 (1997).
[14] M. Miyauchi, A. Nakajima, T. Watanabe, and K. Hashimoto, Chem. Mater. **14**, 2812 (2002).
[15] R. Wang, N. Sakai, A. Fujishima, T. Watanabe, and K. Hashimoto, J. Phys. Chem. B **103**, 2188 (1999).
[16] D. Quere, Rep. Prog. Phys. **68**, 2495 (2005).
[17] R. D. Sun, A. Nakajima, A. Fujishima, T. Watanabe, and K. Hashimoto, J. Phys. Chem. B **105**, 1984 (2001).
[18] H. Nagai, T. Irie, J. Takahashi, S. Wakida, Biosens. Bioelectron. **22**, 1968 (2007).
[19] J. Lahann, S. Mitragotri, T. N. Tran, H. Kaido, J. Sundaram, I. S. Choi, S. Hoffer, G. A. Somorjai, and R. Langer, Science **299**, 371 (2003).
[20] H. Gau, S. Herminghaus, P. Lenz, and R. Lipowsky, Science **283**, 46 (1999).
[21] A. S. Zeng, M. J. Zheng, L. Ma, and W. Z. Shen, Nanotechnology **17**, 4163 (2006).
[22] A. M. Morales and C. M. Lieber, Science **279**, 208 (1998).
[23] Y. Xia, P. Yang, Y. Sun, Y. Wu, B. Mayers, B. Gates, Y. Yin, F. Kim, and H. Yan, Adv. Mater. (Weinheim, Ger.) **15**, 353 (2003).
[24] X. Duan and C. M. Lieber, Adv. Mater. (Weinheim, Ger.) **12**, 298 (2000).
[25] Z. L. Wang, X. Y. Kong, and J. M. Zuo, Phys. Rev. Lett. **91**, 185502 (2003).
[26] S. C. Lyu, Y. Zhang, and C. J. Lee, Chem. Mater. **15**, 3294 (2003).
[27] B. Ozturk, I. Talukdar, and B. N. Flanders, Nanotechnology **18**, 365302 (2007).
[28] Y. X. Liang, S. Q. Li, L. Nie, Y. G. Wang, and T. H. Wang, Appl. Phys. Lett. **88**, 193119 (2006).
[29] A. B. D. Cassie and S. Baxter, Trans. Faraday Soc. **40**, 546 (1944).